

**Negative mobility induced by colored thermal fluctuations**M. Kostur,<sup>1</sup> J. Łuczka,<sup>1</sup> and P. Hänggi<sup>2,3</sup><sup>1</sup>*Institute of Physics, University of Silesia, 40-007 Katowice, Poland*<sup>2</sup>*Institut für Physik, Universität Augsburg, Universitätsstrasse 1, D-86135 Augsburg, Germany*<sup>3</sup>*Department of Physics and Centre for Computational Science and Engineering, National University of Singapore, Singapore 117542, Republic of Singapore*

(Received 8 September 2009; published 20 November 2009)

Anomalous transport of non-Markovian thermal Brownian particle dynamics in spatially periodic symmetric systems that is driven by time-periodic symmetric driving and constant bias is investigated numerically. The Brownian dynamics is modeled by a generalized Langevin equation with exponentially correlated Gaussian thermal noise, obeying the fluctuation-dissipation theorem. We study the role of nonzero correlation time of thermal fluctuations for the occurrence of absolute negative (linear) mobility (ANM) near zero bias, negative-valued, nonlinear mobility (NNM), and negative differential mobility (NDM) at finite bias away from equilibrium. We detect that a nonzero thermal correlation time can either enhance or also diminish the value of ANM. Moreover, finite thermal noise correlation can induce NDM and NNM in regions of parameter space for which such ANM and NNM behaviors are distinctly absent for limiting white thermal noise. In parts of the parameter space, we find a complex structure of regions of linear and nonlinear negative mobility: islands and tongues which emerge and vanish under parameters manipulation. While certain such anomalous transport regimes fade away with increasing temperature some specific regions interestingly remain rather robust. Outside those regimes with anomalous mobility, the ac/dc driven transport is either normal or the driven Brownian particles are not transported at all.

DOI: [10.1103/PhysRevE.80.051121](https://doi.org/10.1103/PhysRevE.80.051121)

PACS number(s): 05.60.-k, 05.45.-a, 85.25.Cp, 74.25.Fy

**I. INTRODUCTION**

Out-of-equilibrium transport processes are of prominent interest in modern statistical physics from all fundamental, experimental, and device aspects [1,2]. A typical far from equilibrium problem is generally nonlinear response of a system to an external stimulus: For example when an external constant force  $F_0$  acts on the system and all other forces are of zero average, it is expected that the long-time stationary average particle velocity  $v$  becomes an increasing function of the load  $F_0$ . An everyday example is that of a force pushing objects on a table. A linear Ohmic resistor characteristic constitutes another example: An increase in voltage is accompanied by a linear increase of current. This normal response behavior is distinct from cases with anomalous transport. Familiar examples are the emergence of negative differential mobility or conductivity [3–5], or the nonlinear response involving negative(-valued) nonlinear mobility away from the linear-response behavior around *zero* applied voltage. Here our focus is on yet another anomalous transport behavior, namely, so-called “absolute negative mobility.” This latter anomalous transport behavior refers to a regime where the resulting velocity or current assumes the opposite sign of the applied force or voltage around the zero-bias regime. While the negative differential mobility (NDM) is common for an abundance of nonlinear systems, the phenomenon of the absolute negative mobility (ANM) has been experimentally detected predominantly much less frequently. Some examples that come to mind are the nonlinear response in  $p$ -modulation-doped GaAs quantum wells [6], or also semiconductor superlattices [7], and recently also in driven Josephson junctions [8]. The phenomenon of ANM can typically relate to a genuine quantum effect, involving

asymmetry tunneling dynamics. In contrast, ANM as a result of classical stochastic dynamics occurs more rare; but it is expected to occur whenever stylized ratchetlike structures including geometric entropic barriers are present. A flurry of recent theoretical [9,10] and some experimental works [8,11] indeed illustrate such behavior.

The effect of ANM can occur also in the form of a far from equilibrium phenomenon in driven nonlinear systems such as in nonlinear underdamped Brownian motion dynamics [12–15] or even in overdamped nonlinear Brownian motion in presence of time-delayed feedback [16].

In this work we shall focus on the case of time-dependent driven underdamped Brownian motion occurring in a periodic reflection symmetric potential and driven by thermal correlated noise. In prior works [12–14], we have studied the transport properties of a classical Brownian particle of mass  $m$  moving in a spatially periodic potential  $V(x)=V(x+L)$  of period  $L$  and barrier height  $\Delta V$ , which is subjected to an external unbiased time-periodic force  $F(t)=F(t+T)$  of period  $T=2\pi/\Omega$  with angular frequency  $\Omega$  and of amplitude  $A$ . Additionally, a constant bias  $F_0$  acts on the system. This so defined Brownian particle dynamics is then modeled by the driven Langevin equation [12], i.e.,

$$m\ddot{x} + \gamma\dot{x} = -V'(x) + A \cos(\Omega t + \phi_0) + F_0 + \xi(t), \quad (1)$$

where  $x=x(t)$  is a position of the particle at time  $t$ , a dot denotes differentiation with respect to time, and a prime denotes a differentiation with respect to the Brownian particle coordinate  $x$ . The parameter  $\gamma$  denotes the viscous friction strength and  $\phi_0$  is an initial phase of the time-periodic driving. Here, the thermal fluctuations are modeled by zero-mean Gaussian white noise  $\xi(t)$  with the Dirac delta autocorrelation function  $\langle \xi(t)\xi(s) \rangle = 2\gamma k_B T_0 \delta(t-s)$ , where  $k_B$  is the

Boltzmann constant and  $T_0$  denotes the temperature.

We could show that in the above system, there are distinct regimes of anomalous transport. In particular we can identify both (i) ANM and (ii) NDM and the phenomenon of (iii) negative nonlinear mobility (NNM), occurring away from the linear-response regime with respect to external bias  $F_0$ . We also remind the reader that Eq. (1) mimics the physical realization for the behavior of a physical Josephson junction [12–15]. In this latter case, the periodic potential  $V(x)$  has the explicit sinusoidal form, i.e.,

$$V(x) = \Delta V \sin(2\pi x/L). \quad (2)$$

Notably, the theoretical findings for ANM in Josephson junctions has recently been verified experimentally with the work in Ref. [8].

The layout of the paper is as follows: In Sec. II, we present the generalized Langevin equation determining dynamics of the Brownian particle in presence of exponentially correlated thermal fluctuations. Next, in Sec. III, we address the problem of influence of correlated thermal fluctuations on both ANM and NNM. In the parameter space, we reveal a refined structure of regions of negative mobility. Outside these regions, transport is normal or particles are not transported at all. We find that small nonzero correlation time does not destroy ANM within tailored parameter regimes studied previously in the context of current-voltage characteristics of a Josephson-junction device. Section IV provides summary and some conclusions.

## II. PERIODICALLY DRIVEN AND BIASED NON-MARKOVIAN BROWNIAN DYNAMICS

The thermal noise  $\xi(t)$  in Eq. (1) is approximated to be ideally white noise with zero noise correlation time  $\tau_c=0$ . In real systems, however, the correlation time of thermal fluctuations is only approximately zero. This approximation is justified if  $\tau_c$  is much smaller than the smallest characteristic time  $\tau_s$  of the system itself. There are many examples where this situation is well satisfied in real systems. There are, however, also situations where the thermal correlation time  $\tau_c$  is of order or greater than  $\tau_s$ , so that the white-noise approximation fails [17–19]. In this latter case a modeling based on the Markovian Langevin Eq. (1) is not correct; instead, the generalized Langevin equation should then be invoked.

### A. Generalized Langevin dynamics

When the thermal noise is correlated, the appropriate Langevin dynamics is a non-Markovian dynamics with memory friction described by the so-called generalized Langevin equation (GLE) [20–24]. It explicitly reads

$$m\ddot{x}(t) + \int_0^t K(t-s)\dot{x}(s)ds = -U'(x(t),t) + \xi(t), \quad (3)$$

where the full potential takes the form

$$U(x,t) = V(x) - [A \cos(\Omega t + \phi_0) + F_0]x. \quad (4)$$

This non-Markovian dynamics can be derived from first principles by means of coupling the system of interest to a

bath of harmonic oscillators [21,23] with the total system being prepared in canonical thermal equilibrium [23]. It then follows from the central limit theorem that the thermal fluctuations  $\xi(t)$  obey a zero-mean stationary typically non-Markovian Gaussian stochastic process. The autocorrelation function of the thermal noise  $\xi(t)$  is related to the memory (frictional) kernel  $K(t)$  via the fluctuation-dissipation relation [20–24],

$$\langle \xi(t)\xi(s) \rangle = k_B T_0 K(|t-s|). \quad (5)$$

Interestingly, due to the nonlinearity of the potential  $V(x)$  it is still an unsolved open problem to derive the explicit form of the generalized master equation for the single-event non-Markovian probability  $p(x, \dot{x}, t)$ , see in Refs. [22,23,25]; this task is achieved only in form of a time-convolutionless master equation with time-dependent transport coefficients if the potential  $V(x)$  is at most quadratic in  $x$  only [23,25]. The approach yields a general non-Markovian Gauss process for the equilibrium dynamics  $[x(t), \dot{x}(t)]$ .

### B. Exponentially correlated thermal fluctuations

The Gaussian thermal fluctuations  $\xi(t)$  in Eq. (3) are completely determined by the memory function  $K(t)$ . If the memory function  $K(t)$  is the Dirac delta function, i.e.,  $K(t) = 2\gamma\delta(t)$ , then Eq. (3) reduces to the form (1). A well-studied form of correlated fluctuations is defined by means of an Ornstein-Uhlenbeck (O-U) stationary stochastic process for  $\xi(t)$  [18]. This Gaussian Markov process for the thermal noise (note that the resulting Brownian dynamics is then still non-Markovian) is henceforth correlated exponentially. We next use a Markovian embedding of the GLE dynamics in Eq. (3). Toward this objective we present the correlation function in the form

$$\langle \xi(t)\xi(s) \rangle = k_B T_0 K(|t-s|) = \frac{\gamma k_B T_0}{\tau_c} e^{-|t-s|/\tau_c}, \quad (6)$$

where  $\tau_c$  is the correlation time of the O-U process which we can then smoothly vary from the limit of white Gaussian noise ( $\tau_c=0$ ) to strongly correlated thermal noise ( $\tau_c \gg \tau_s$ ). Because the integral kernel exhibits an exponential form, we can convert Eq. (3) into a set of ordinary stochastic differential equations: Let us define the auxiliary stochastic process  $w(t)$  via the relation

$$w(t) = \frac{\gamma}{\tau_c} \int_0^t e^{-(t-s)/\tau_c} \dot{x}(s) ds. \quad (7)$$

Then Eq. (3) is equivalently transformed into the form

$$m\dot{w}(t) = -U'(x(t),t) - w(t) + \xi(t), \quad (8)$$

$$\dot{x}(t) = v(t), \quad (9)$$

$$\dot{w}(t) = -\frac{1}{\tau_c} w(t) + \frac{\gamma}{\tau_c} v(t), \quad (10)$$

$$\dot{\xi}(t) = -\frac{1}{\tau_c}\xi(t) + \frac{1}{\tau_c}\sqrt{2\gamma k_B T_0}\Gamma(t), \quad (11)$$

where the normalized white Gaussian noise  $\Gamma(t)$  obeys  $\langle \Gamma(t)\Gamma(s) \rangle = \delta(t-s)$  while the last equation of this set describes the O-U noise with the exponential correlation function (6) [26,27]. Note that in Eq. (8), the linear combination  $z(t) = \xi(t) - w(t)$  occurs. By subtracting the two last relation we then find the set of three coupled Markovian Langevin equations, modeling the two-dimensional non-Markovian GLE in Eq. (3), i.e.,

$$\dot{x}(t) = v(t), \quad (12)$$

$$\dot{v}(t) = -\frac{1}{m}U'(x(t), t) + \frac{1}{m}z(t), \quad (13)$$

$$\dot{z}(t) = -\frac{1}{\tau_c}z(t) - \frac{\gamma}{\tau_c}v(t) + \frac{1}{\tau_c}\sqrt{2\gamma k_B T_0}\Gamma(t). \quad (14)$$

The corresponding three-dimensional Fokker-Planck equation for  $p(x, v, z, t)$  is numerically cumbersome to implement for  $V(x)$  a nonlinear spatially periodic function. Alternatively we apply direct numerical methods for the solution of the three coupled Langevin equations in Eqs. (12)–(14).

The limiting case of white noise has been analyzed in detail in Refs. [12–14], where a numerical method has been described, see also in Refs. [28,29]. In the remaining of this work we shall use the dimensionless form of the set of Eqs. (12)–(14). In doing so we scale coordinate  $x$  and time  $t$  as follows:

$$X = \frac{x}{L}, \quad \hat{t} = \frac{t}{\tau_0}, \quad \tau_0^2 = \frac{mL^2}{\Delta V}. \quad (15)$$

Then, the set of Eqs. (12)–(14) is recast as

$$\dot{X} = Y, \quad (16)$$

$$\dot{Y} = -W'(X) + a \cos(\omega\hat{t} + \phi_0) + f + Z, \quad (17)$$

$$\dot{Z} = -\frac{1}{\hat{\tau}_c}Z - \frac{\hat{\gamma}}{\hat{\tau}_c}Y + \frac{1}{\hat{\tau}_c}\sqrt{2\hat{\gamma}D}\hat{\xi}(\hat{t}), \quad (18)$$

where

$$Y = \frac{\tau_0}{L}v, \quad Z = \frac{L}{\Delta V}z \quad (19)$$

and a dot denotes differentiation with respect to the rescaled time  $\hat{t}$ . Here,  $Y = Y(\hat{t})$  is the dimensionless velocity of the Brownian particle and  $Z = Z(\hat{t})$  denotes the corresponding dimensionless random force. The remaining rescaled parameters are: (1) the friction coefficient  $\hat{\gamma} = (\gamma/m)\tau_0 = \tau_0/\tau_L$  equals the ratio of two characteristic times, namely, time  $\tau_0$  and the relaxation time of the velocity degree of freedom, i.e.,  $\tau_L = m/\gamma$ ; (2) the correlation time  $\hat{\tau}_c = \tau_c/\tau_0$ ; (3) the potential  $W(X) = V(x)/\Delta V = W(X+1) = \sin(2\pi X)$  possesses unit period and barrier height  $\Delta\hat{V} = 2$ ; (4) the amplitude  $a = LA/\Delta V$  and the frequency  $\omega = \Omega\tau_0$  (or the period  $\mathcal{T}$

$= 2\pi/\omega$ ); (5) the load  $f = LF_0/\Delta V$ ; (6) the zero-mean white noise  $\hat{\xi}(\hat{t})$  is correlated as  $\langle \hat{\xi}(\hat{t})\hat{\xi}(\hat{s}) \rangle = \delta(\hat{t}-\hat{s})$  with a rescaled noise intensity  $D = k_B T_0/\Delta V$ . The latter is given as the ratio of two energies, thermal energy, and half of barrier height of the potential  $V(x)$ .

From here on, we shall use only these dimensionless variables and shall omit the notation “hat” in all quantities in Eqs. (16)–(18).

### III. NUMERICAL RESULTS FOR BROWNIAN NON-MARKOVIAN ANOMALOUS TRANSPORT

We next study numerically the long-time transport characteristics of the nonlinear Brownian dynamics with memory friction. In particular we shall focus on the current feature as given by the long-time averaged velocity  $v \equiv \langle Y \rangle$ . This averaging is performed as follows: First we perform an average over all realizations of the thermal fluctuations which yields a temporally varying quantity. A second temporal average is over the cycle period of the external ac driving. Because the resulting asymptotic long-time dynamics is not necessarily ergodic (i.e., independent of chosen initial conditions) in all phase space we also need to perform an average over unbiased initial conditions. We have chosen uniformly distributed initial positions  $X(t=0) = X_0$  over one period of the periodic potential  $W(X)$ ; the initial velocities  $Y(t=0) = Y_0$  are unbiased and taken as uniformly distributed in the interval  $[-2, 2]$  and the initial phase  $\phi_0 \in [0, 2\pi]$ . The symmetry consideration of Eq. (3) then implies that this average velocity  $v(f)$  as a function of the external constant force  $f$  is an odd function, i.e.,  $v(-f) = -v(f)$ ; thus  $v(f=0) = 0$ . Therefore we will in our numerics only consider the half-axis with  $f \geq 0$ .

We have used the Stochastic Runge-Kutta algorithm of the second order [30] with a time step typically  $10^{-3}$  (for small correlation times  $\tau$  smaller time steps were taken). All calculations have been performed on Nvidia Tesla C1060 using CUDA environment, which accelerated the speed of simulations by almost three orders of magnitudes compared to CPU implementation. The detailed description of the implementation can be found in [31].

Because, as showed with previous works with white thermal noise [12–15], the transport dynamics becomes very rich indeed in the parameter space exhibiting all, namely, ANM, NDM, and NNM. As it must be expected this richness does not diminish with yet another parameter of variation, namely, the correlation time of thermal noise  $\tau_c$ . Also it must be kept in mind that it is impossible to scan numerically over *all* possible parameter space of the driven nonlinear Brownian dynamics. In the following we shall focus our numerical study to regimes in parameter space that are (i) experimentally accessible [12–14] and (ii) exhibit a peculiar complexity for the nonlinear response.

Clearly, the resulting velocity  $v = v(f)$  is typically nonlinear in external bias  $f$ . The linear-response behavior is defined for small bias  $f \rightarrow 0$  as

$$v(f \rightarrow 0) = \mu f, \quad (20)$$

where the (linear) mobility  $\mu$  can become negative,  $\mu < 0$ . This regime will be termed absolute negative mobility

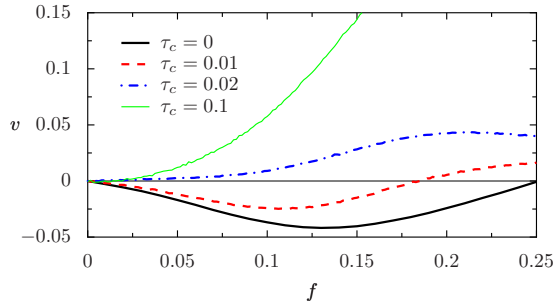


FIG. 1. (Color online) Illustration of destructive role of finite thermal noise correlations on absolute negative mobility (ANM): The averaged long-time velocity  $v$  of the ac driven Brownian particle is depicted as a function of the externally applied, static force  $f$ . The chosen system parameters are  $a=4.578$ ,  $\omega=4.9$ ,  $\gamma=0.9$ , and  $D=0.001$ . While white thermal noise ( $\tau_c=0$ ) does depict ANM this is increasingly diminished upon increasing the correlation time of thermal noise until it merges into a normal positive mobility behavior.

(ANM); i.e., an anomalous transport regime for which the particle is transported in the *opposite direction* to the externally applied force  $f$ . Moreover, negative nonlinear mobility (NNM) refers to an anomalous transport regime for which we find  $v(f)/f < 0$  in some finite intervals of  $f$ , being disjoint from the interval around  $f=0$ . Finally, regimes of negative differential mobility (NDM), when  $dv(f)/df < 0$  in some intervals of  $f$ , can be detected.

## A. Controlling ANM with noise correlation time

### 1. Undoing ANM with small noise correlation time

We first consider small bias values  $f$  and study the linear ( $f \rightarrow 0$ ) response and the accompanying nonlinear response with increasing  $f$  to larger values for specific parameter settings. We first zoom into a parameter regime for which we find ANM for  $\tau_c=0$ . An example is depicted with Fig. 1. If the correlation time  $\tau_c$  increases, starting out from zero, we observe a diminishing ANM with increasing  $\tau_c$ , until it disappears and turns into normal positive-valued mobility upon increasing  $\tau_c$  further. Put differently, the mobility coefficient  $\mu$  in Eq. (20) starts to increase from negative values, passes through zero, and eventually becomes positive. For  $\tau_c > 0.035$ , the velocity monotonically increases in the region of small bias  $f$  with  $\mu > 0$ . Note that the dimensionless correlation time is rather short in comparison to the other characteristic time scales, that is with the characteristic time scale  $\tau_0=1$ , the characteristic velocity relaxation time scale  $1/\hat{\gamma}=1.11\tau_0$ , and the period of the driving force  $T=1.28\tau_0$ .

A first main finding therefore is that even a small finite thermal noise correlation time can diminish and even undo ANM.

### 2. Enhancing ANM and creating NNM

Upon scanning the parameter set to a different forcing strength of the ac driving we find that thermal noise correlations can in fact also *enhance* rather than diminish the value of ANM. This is illustrated in Fig. 2, panel (a), for noise

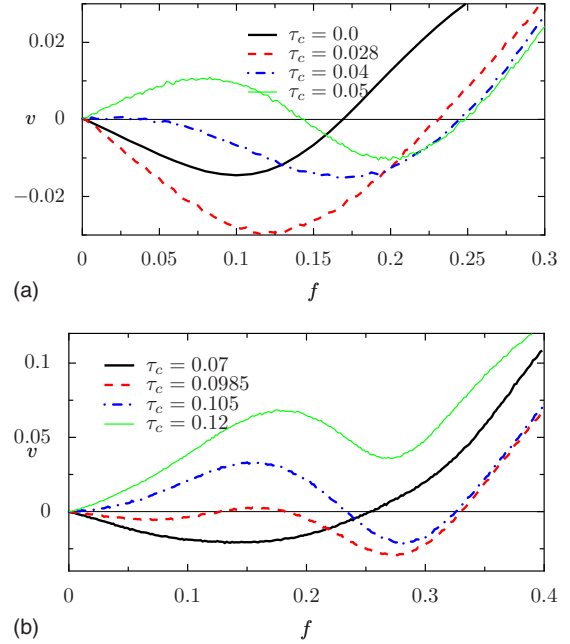


FIG. 2. (Color online) Illustration of constructive role of thermal noise correlations on absolute negative mobility: The averaged long-time velocity  $v$  of the Brownian particle is depicted as a function of the bias force  $f$  for selected values of the noise correlation time  $\tau_c$  of thermal fluctuations. The system parameters are different from Fig. 1 and read  $a=4.1293$ ,  $\omega=4.9$ ,  $\gamma=0.9$ , and  $D=0.001$ . (a) Within this regime we find that a small thermal noise correlation time can *enhance* ANM. (b) Upon further increasing thermal noise correlation time  $\tau_c$  from the values shown in (a) we observe a turnover into ANM again (case  $\tau_c=0.07$ ); followed by a NNM behavior ( $\tau_c=0.0985$ ). Finally reentry into a normal transport regime is observed at small bias with a regime exhibiting NDM as  $f$  is increased further ( $\tau_c=0.12$ ).

correlation times varying in the interval  $\tau_c \in [0, 0.028]$ . Beyond  $\tau_c=0.028$  ANM diminishes again, exhibiting also regimes with NNM ( $\tau_c=0.05$ ).

It is intriguing to note that within this parameter setting a further increase in the correlation time yields an opposite behavior, see panel (b) in Fig. 2. The mobility coefficient  $\mu$  then is decreasing from positive values and next turns into ANM again. The most pronounced ANM value occurs around  $\tau_c=0.08$  (not shown) before entering a regime with coexistence of both ANM and NNM around  $\tau_c=0.1$ . For larger correlation time we find normal linear mobility followed up in the nonlinear regime with a region exhibiting NDM.

We note that the various situations described above do occur and can coexist in other settings of the parameters.

## B. Correlation time induced Islands and tongues of ANM and NNM

While in the previous subsection we have varied the external bias  $f$  away from zero we next keep this bias *fixed* at  $f=0.1$  and scan instead the correlation time  $\tau_c$  versus the ac-driving strength  $a$ . The emerging asymptotic averaged velocities are then depicted in color-coded plots as shown in



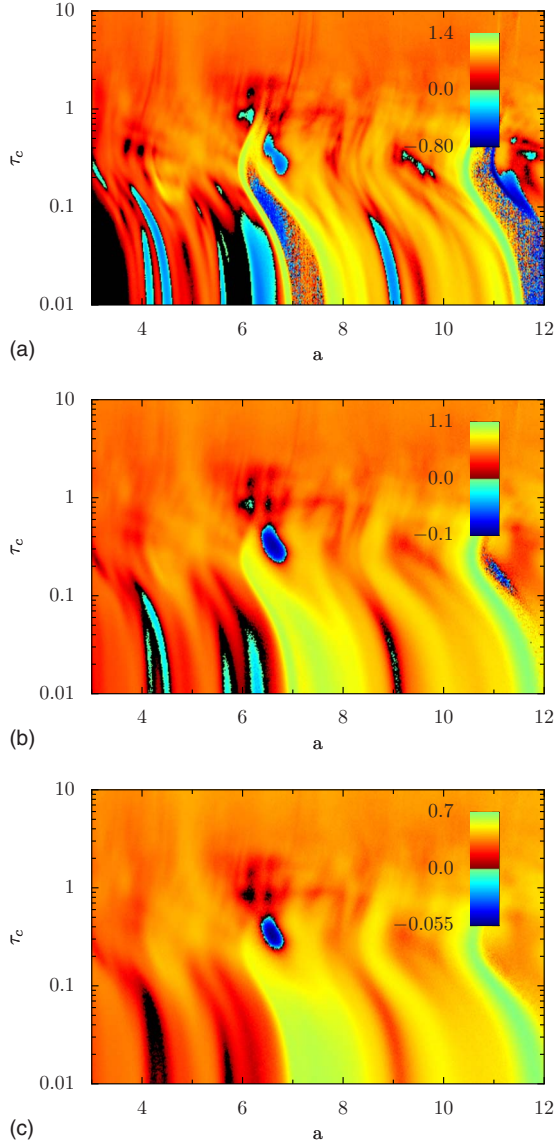


FIG. 3. (Color online) Regions of negative (nonlinear) mobility manifested either as ANM or also NNM, in the parameter plane given by  $\{a, \tau_c\}$  for three different temperatures,  $D=0.0001, 0.001, 0.01$  (top to bottom). The remaining parameters are fixed: namely,  $a=4.1293$ ,  $\omega=4.9$ ,  $\gamma=0.9$ , and  $f=0.1$ .

Fig. 3 for three different settings of the temperature  $T_0$ . Our comprehensive numerical investigations reveal a rich diversity of structures, formed by regions of both, ANM and NNM. In Fig. 3, we depict how the parameter plane  $\{a, \tau_c\}$  is divided into regions of normal [ $v(f) > 0$  for  $f > 0$ ] and anomalous [ $v(f) < 0$  for  $f > 0$ ] transport. In doing so here we do not discriminate between ANM and NNM. Both these transport behaviors are jointly presented. Not unexpected, there occur in this parameter plane several domains with anomalous transport features. The geometric structure of these domains in the depicted regime of the  $\{a, \tau_c\}$  variation is very complex. Let us remind ourselves that the underlying deterministic dynamics is chaotic in some regimes and therefore fractal structures of certain domains must be expected to exist. We are interested in the stability of those domains in parameter space for which ANM and/or NNM occur. Two

thermal situations, namely, “low” and “high” temperatures are shown for comparison. At low temperature, cf. the upper panel, we reveal the refined structure with many narrow, slim, and twisted regions of ANM-NNM. Some of those regions, the “tongues,” survive with correlation time  $\tau_c$  approaching zero (i.e., the horizontal abscissa) and there are “islands” of negative mobility which disappear for  $\tau_c=0$ . If one fixes one of the parameters, say  $\tau_c=0.1$ , intervals of negative mobility are clearly noticeable: there are several intervals of the amplitude  $a \in (a_i, a_{i+1})$  for which ANM-NNM can be detected. Outside these intervals, a normal response to the load  $f$  is found.

If temperature is increased, this small temperature structure is increasingly washed out; i.e., it becomes smoother. Many previously existing domains of ANM-NNM behavior start to shrink or vanish altogether. We detect a few robust regimes for which anomalous transport persists, namely, a few islands and a few tongues. The most robust such island against increasing noise strength (temperature) is the island located around  $\{a, \tau_c\} = \{6.56, 0.31\}$ . This domain even survives at high temperatures.

We emphasize that such complicated regimes of ANM-NNM are not just rare occurrences: they can be verified with numerically arbitrarily-high-accuracy calculations and over extended intervals in parameter space. Given the complexity of the underlying dynamics with time-dependent ac driving nonlinearity and in presence of noise with finite correlation time, the observed behavior is clearly beyond a sensible analytical description.

### C. Current-voltage characteristics of a realistic Josephson-junction device

As an application of the above theoretical study we consider next a Josephson junction for which the anomalous conductance has been measured in Ref. [8]. The relation in Eq. (1) with the potential (2) models the resistively and capacitively shunted Josephson junction, also known as the Stewart-McCumber model [32–34]. It contains three additive current contributions: a Cooper pair tunnel current characterized by the critical current  $I_0$ , a normal (Ohmic) current characterized by the normal-state resistance  $R$ , and a displacement current due to the capacitance  $C$  of the junction. For this model, the position  $x$  of the Brownian particle translates into is the phase difference  $\phi$  between the macroscopic wave functions of the Cooper pairs on both sides of the junction, i.e.,  $x = \phi$ , the mass  $m = (\hbar/2e)^2 C$ , the friction coefficient  $\gamma = (\hbar/2e)^2 (1/R)$ , the barrier height  $\Delta V = (\hbar/2e) I_0$  and the period  $L = 2\pi$ . The load  $F_0 = (\hbar/2e) I_d$  is given by means of the dc-bias current, the amplitude  $A = (\hbar/2e) I_a$ , and the frequency  $\Omega$  define the external ac current. The velocity  $v = \dot{x}$  translates into the voltage across the junction. The experimental results for the Josephson junction presented in Ref. [8] show very good agreement with the Stewart-McCumber model with the following set of parameter values: namely, the dimensionless amplitude of the ac current  $a = 13.874$ , the frequency  $\omega = 2.75$ , the friction coefficient  $\gamma = 2.264$ , and the (white) noise intensity  $D = 0.000895$ . We note that Eq. (3) can serve as a generalization of the Stewart-McCumber

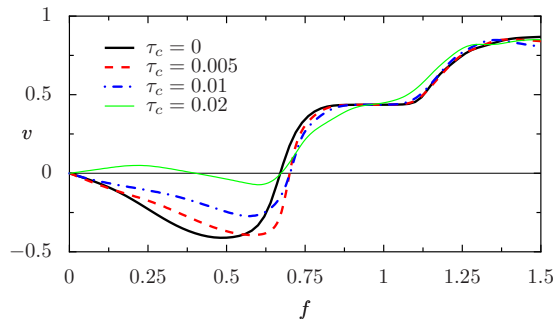


FIG. 4. (Color online) Role of nonzero thermal noise correlations on absolute negative mobility for a parameter set corresponding to the anomalous Josephson-junction transport regime used in the experiment in Ref. [8]. The long-time averaged voltage  $v$  across the junction is depicted as a function of the externally applied dc current  $f$ . The corresponding dimensionless parameters are  $a = 13.874$ ,  $\omega = 2.75$ ,  $\gamma = 2.264$ , and  $D = 0.000\ 895$ . The white thermal noise regime (i.e.,  $\tau_c = 0$ ) depicts ANM behavior which is sustained for short correlation times of the thermal noise. For increasingly larger correlation times ANM is diminished and eventually vanishes all together and crosses over into a normal positive mobility behavior. Still, negative-valued, nonlinear mobility can occur far away from equilibrium; note the nonlinear response behavior for  $\tau = 0.02$  and around  $f \sim 0.6$ .

model toward a regime of validity to lower temperatures where finite correlations of the thermal fluctuations increasingly play a significant role [34]. We numerically find that at small nonzero correlation time of the thermal fluctuations ANM is sustained within tailored parameter regimes, as studied previously in the context of current-voltage characteristics of a ac driven Josephson-junction device in Ref. [8], see Fig. 4. With increasing thermal noise correlation time ANM is weakened and finally turns into normal behavior followed by a regime of NNM far away from equilibrium. This feature of finite thermal noise correlation is of relevance from an experimental point of view when measuring mobility as a function of temperature. We can also conclude from this study that at the temperature of the experiment performed in Ref. [8], the white thermal noise approximation is seemingly well satisfied.

#### IV. CONCLUSIONS

With this study we numerically analyzed the role of nonzero correlation time of thermal fluctuations on the anomalous transport regimes of underdamped non-Markovian Brownian particles that are driven by time-periodic and static forces. We detected a rich variety of anomalous transport behavior in an experimentally wide parameter space where anomalous transport can be monitored. The regions of absolute negative mobility and negative nonlinear mobility form complicated structures in parameter space with stripes, fibers, and islands, see Fig. 3. At low temperatures these structures can unambiguously be attributed to finite correlations of thermal fluctuations. Such correlations are either constructive or destructive in nature with respect to the size of anomalous transport coefficients such as mobility. A subsequent increase of temperature tends to blur these structures. Nevertheless, there occur stable “islands” with anomalous negative-valued mobility behavior which are solely induced by nonzero thermal noise correlations (Fig. 3).

In the regime of linear mobility response, such nonzero thermal correlations are found either to diminish or also to enhance the regime of absolute negative (linear) mobility, dependent on the specific parameter setting for ac-driving strength and/or remaining parameters.

We also have compared our predictions in a parameter regime of a recent experiment on anomalous response behavior in a ac/dc driven Josephson junction [8]: The observed ANM behavior is sustained for small thermal noise correlation time but increasingly fades out with increasing thermal noise correlation (in Fig. 4).

#### ACKNOWLEDGMENTS

Work supported by DAAD (J.L.), the Polish Ministry of Science and Higher Education under Grant No. 202 203 534, the German Excellence Initiative via the “Nanosystems Initiative Munich (NIM),” and by the DFG through the collaborative research center SFB-486.

- 
- [1] P. Hänggi and F. Marchesoni, *Rev. Mod. Phys.* **81**, 387 (2009).
  - [2] R. D. Astumian and P. Hänggi, *Phys. Today* **55** (11), 33 (2002).
  - [3] A. Sibille, J. F. Palmier, H. Wang, and F. Mollot, *Phys. Rev. Lett.* **64**, 52 (1990).
  - [4] S. M. Sze and Kwok K. Ng, *Physics of Semiconductor Devices* (Wiley, NY, 2007).
  - [5] S. Martens, D. Hennig, S. Fugmann, and L. Schimansky-Geier, *Phys. Rev. E* **78**, 041121 (2008).
  - [6] R. A. Höpfel, J. Shah, P. A. Wolff, and A. C. Gossard, *Phys. Rev. Lett.* **56**, 2736 (1986).
  - [7] B. J. Keay, S. Zeuner, S. J. Allen, Jr., K. D. Maranowski, A. C. Gossard, U. Bhattacharya, and M. J. W. Rodwell, *Phys. Rev. Lett.* **75**, 4102 (1995); E. H. Cannon, F. V. Kusmartsev, K. N. Alekseev, and D. K. Campbell, *ibid.* **85**, 1302 (2000).
  - [8] J. Nagel, D. Speer, T. Gaber, A. Sterck, R. Eichhorn, P. Reimann, K. Ilin, M. Siegel, D. Koelle, and R. Kleiner, *Phys. Rev. Lett.* **100**, 217001 (2008).
  - [9] R. Eichhorn, P. Reimann, and P. Hänggi, *Phys. Rev. Lett.* **88**, 190601 (2002).
  - [10] R. Eichhorn, P. Reimann, and P. Hänggi, *Phys. Rev. E* **66**, 066132 (2002); *Physica A* **325**, 101 (2003); R. Eichhorn, P. Reimann, B. Cleuren, and C. Van den Broeck, *Chaos* **15**, 026113 (2005).
  - [11] A. Ros, R. Eichhorn, J. Regtmeier, T. T. Duong, P. Reimann, and D. Anselmetti, *Nature (London)* **436**, 928 (2005).
  - [12] L. Machura, M. Kostur, P. Talkner, J. Łuczka, and P. Hänggi, *Phys. Rev. Lett.* **98**, 040601 (2007).

- [13] M. Kostur, L. Machura, P. Talkner, P. Hänggi, and J. Łuczka, Phys. Rev. B **77**, 104509 (2008); Physica E (to be published).
- [14] L. Machura, M. Kostur, J. Łuczka, P. Talkner, and P. Hänggi, Acta Phys. Pol. B **39**, 1115 (2008).
- [15] D. Speer, R. Eichhorn, and P. Reimann, Phys. Rev. E **76**, 051110 (2007).
- [16] D. Hennig, Phys. Rev. E **79**, 041114 (2009).
- [17] P. Hänggi and P. Jung, Adv. Chem. Phys. **89**, 239 (1995).
- [18] J. Łuczka, Chaos **15**, 026107 (2005).
- [19] I. Goychuk and P. Hänggi, Adv. Phys. **54**, 525 (2005).
- [20] R. Kubo, Rep. Prog. Phys. **29**, 255 (1966).
- [21] R. Zwanzig, J. Stat. Phys. **9**, 215 (1973).
- [22] H. Grabert, P. Hänggi, and P. Talkner, J. Stat. Phys. **22**, 537 (1980).
- [23] P. Hänggi, Lect. Notes Phys. **484**, 15 (1997).
- [24] P. Hänggi, P. Talkner, and M. Borkovec, Rev. Mod. Phys. **62**, 251 (1990).
- [25] P. Hänggi, Z. Phys. B **31**, 407 (1978).
- [26] J. Łuczka, Physica A **153**, 619 (1988); J. Łuczka, M. Niemiec, and E. Piotrowski, Phys. Lett. A **167**, 475 (1992).
- [27] P. Jung and P. Hänggi, Phys. Rev. Lett. **61**, 11 (1988).
- [28] L. Machura, M. Kostur, F. Marchesoni, P. Talkner, P. Hänggi, and J. Łuczka, J. Phys.: Condens. Matter **17**, S3741 (2005).
- [29] L. Machura, M. Kostur, P. Talkner, J. Łuczka, F. Marchesoni, and P. Hänggi, Phys. Rev. E **70**, 061105 (2004).
- [30] R. L. Honeycutt, Phys. Rev. A **45**, 600 (1992).
- [31] M. Januszewski and M. Kostur, Comput. Phys. Commun. (to be published).
- [32] W. C. Stewart, Appl. Phys. Lett. **12**, 277 (1968).
- [33] D. E. McCumber, J. Appl. Phys. **39**, 3113 (1968).
- [34] R. L. Kautz, Rep. Prog. Phys. **59**, 935 (1996).